

# Glass forming ability of Fe–Co–Zr–Nd–B alloys and bulk permanent magnets derived from amorphous precursor

X. H. Tan · H. Xu · S. J. Wu

Received: 20 January 2010 / Accepted: 11 May 2010 / Published online: 21 May 2010  
© Springer Science+Business Media, LLC 2010

**Abstract** The glass forming ability (GFA) and magnetic properties for  $\text{Fe}_{48-x}\text{Co}_{27}\text{Zr}_3\text{Nd}_x\text{B}_{22}$  ( $x = 0-6$ ) alloys were investigated. It was found that the proper addition of Nd (4–5 at.%) was very effective in improving GFA. The as-cast  $\text{Fe}_{44}\text{Co}_{27}\text{Zr}_3\text{Nd}_4\text{B}_{22}$  and  $\text{Fe}_{43}\text{Co}_{27}\text{Zr}_3\text{Nd}_5\text{B}_{22}$  alloys exhibited good soft magnetic behavior, while showed hard magnetic property after annealing at 760 °C for 10 min. Bulk permanent magnets were obtained from crystallization of amorphous alloys, which could provide a promising way for the bulk magnet produced by the simple process of copper mold casting and subsequent heat treatment.

## Introduction

Metallic glasses with unique mechanical and physical properties are believed to have considerable application potentials as advanced engineering and functional materials [1–9]. Since the amorphous Fe–P–C alloy prepared by rapid solidification technique in 1967 [10], Fe-based amorphous ferromagnetic alloys are being investigated for their promising use in electrical devices. However, these alloys have usually been prepared in ribbon form and wire form because of their poor glass forming ability (GFA), leading to the restriction of their application fields [11, 12]. Therefore, it is desired to develop Fe-based alloy with high GFA to extend their industrial applications. Since 1995, a series of Fe-based bulk metallic glasses (BMGs) with high GFA and good soft ferromagnetic properties have been found [13–20]. In 2000, on the basis of Nd–Fe–B-

based alloy, Zhang and Inoue [21] reported that fully dense  $\text{Nd}_2\text{Fe}_{14}\text{B}/(\text{Fe}_3\text{B}, \alpha\text{-Fe})$  nanocomposite permanent magnet could be produced by crystallization of bulk glassy  $\text{Fe}_{67}\text{Co}_{9.4}\text{Nd}_{3.1}\text{Dy}_{0.5}\text{B}_{20}$  alloy. The hard behavior is due to the ferromagnetic exchange coupling between magnetically soft and hard phases. Traditionally, Nd–Fe–B permanent magnets are produced by melt spinning or mechanical alloying. Several steps are required to obtain a final product with optimal magnetic properties, which has disadvantages of high manufacturing cost and long production time. The significance of Zhang's work is that they provide one promising way for the bulk magnet produced by the simple process of copper mold casting and subsequent heat treatment, which extends the applications of Fe-based BMGs as important functional materials.

Zhang's method included two points. That is, BMGs were got first and then bulk permanent alloys could be obtained after the heat treatment of glassy alloys. In our previous work [22–24], bulk  $\text{Fe}_{61}\text{Co}_{10}\text{Nd}_3\text{Y}_6\text{B}_{20}$  and  $\text{Fe}_{68}\text{Zr}_2\text{Nd}_5\text{Y}_4\text{B}_{21}$  permanent magnets had been made by this way. However, the GFA of  $\text{Fe}_{61}\text{Co}_{10}\text{Nd}_3\text{Y}_6\text{B}_{20}$  and  $\text{Fe}_{68}\text{Zr}_2\text{Nd}_5\text{Y}_4\text{B}_{21}$  alloys are not good enough to get BMGs with large size, which triggers us to find more Fe-based systems with high GFA and synthesize the permanent magnet in a bulk form by crystallization amorphous alloys. Based on Fe–Co–Zr–B alloy, a series of BMGs had been formed by minor addition [14, 25, 26]. However, they exhibited soft magnetic properties for as-cast state or annealing state.

In this work, the GFA and magnetic properties for Fe–Co–Zr–Nd–B alloys were investigated. Nd was selected as candidate element because it satisfied the empirical rules for the achievement of Fe-based BMGs with high GFA [27, 28]. Furthermore, by adding Nd to the Fe–Co–Zr–B system,  $\text{Nd}_2\text{Fe}_{14}\text{B}$  phase might be formed and

X. H. Tan (✉) · H. Xu · S. J. Wu  
Institute of Material Science, Shanghai University,  
Yanchang Road, Shanghai 200072, People's Republic of China  
e-mail: tanxiaohua123@shu.edu.cn; tanxiaohua123@163.com

expected to make alloys exhibit hard magnetic property after heat treatment.

## Experimental

### Materials

The  $\text{Fe}_{48-x}\text{Co}_{27}\text{Zr}_3\text{Nd}_x\text{B}_{22}$  ( $x = 0-6$ ) alloy ingots were prepared by arc melting mixtures of pure metals Fe, Co, Zr, Nd, and Fe–B alloy under argon atmosphere. The ingots were melted four times to ensure homogeneity. Bulk sheet specimens (1 mm × 10 mm × 80 mm) were prepared by suction casting of the molten alloy into a copper mold. The samples were annealed in a furnace with a vacuum of  $2 \times 10^{-3}$  Pa at 760 °C for 10 min.

### Characterization

Structural investigations of the as-cast and annealed samples were monitored by X-ray diffraction (XRD) in a Siemens D5000 diffractometry using Cu K $\alpha$  radiation. The thermal behavior of alloys was measured using differential scanning calorimetry (DSC) under argon atmosphere at a heating rate of 20 °C/min. Magnetic properties of the alloys were measured using a vibrating sample magnetometer with a maximum applied field of 1.8 T at room temperature.

## Results and discussion

### Glass forming ability

Figure 1 shows XRD spectra of as-cast  $\text{Fe}_{48-x}\text{Co}_{27}\text{Zr}_3\text{Nd}_x\text{B}_{22}$  ( $x = 0-6$ ) samples. For the  $\text{Fe}_{48}\text{Co}_{27}\text{Zr}_3\text{B}_{22}$  ( $x = 0$ ) alloy, the specimen exhibits sharp crystalline peaks

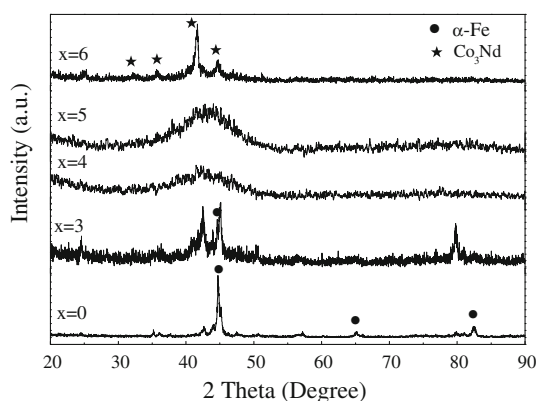


**Fig. 1** XRD patterns for  $\text{Fe}_{48-x}\text{Co}_{27}\text{Zr}_3\text{Nd}_x\text{B}_{22}$  ( $x = 0-6$ ) alloys prepared by suction casting

which identified  $\alpha$ -Fe phase. When Nd content reaches 3 at.%,  $\alpha$ -Fe peak is depressed. XRD patterns for  $x = 4$  and  $x = 5$  samples reveal the characteristic broad diffraction peaks typical of a fully amorphous structure, which indicates bulk amorphous  $\text{Fe}_{44}\text{Co}_{27}\text{Zr}_3\text{Nd}_4\text{B}_{22}$  and  $\text{Fe}_{43}\text{Co}_{27}\text{Zr}_3\text{Nd}_5\text{B}_{22}$  alloys are formed in Fe–Co–Zr–Nd–B system. However, with a further increase Nd content to 6 at.%, the XRD pattern exhibits sharp peaks indicating the formation of  $\text{Co}_3\text{Nd}$  phase. Therefore, it may be deduced that the proper addition of Nd (4–5 at.%) is very effective in improving the GFA of Fe–Co–Zr–Nd–B alloys.

The DSC curves recorded at a constant heating rate of 20 °C/min for  $\text{Fe}_{48-x}\text{Co}_{27}\text{Zr}_3\text{Nd}_x\text{B}_{22}$  ( $x = 3-6$ ) alloys are shown in Fig. 2. The obvious exothermic peaks caused by crystallization are observed for all samples. As marked with arrows, the offset crystallization temperature ( $T_x$ ) increases from 631 °C at  $x = 3$  at.% to 662 °C at  $x = 6$  at.%, indicating that the thermal stability of the amorphous alloys increases with the addition of Nd. The values of  $T_x$  are shown in Table 1. However, neither appreciable endothermic reaction due to glass transition nor the subsequent supercooled liquid region before crystallization is observed, which is similar to what occurs for ( $\text{Fe}_{71.2}\text{B}_{24}\text{Y}_{4.8}$ ) $_{96}\text{Nb}_4$  and Fe–Co–Pt–B alloy [29, 30].

It is known that the GFA of metallic alloys is generally characterized by the supercooled liquid region,  $\Delta T_x = T_x - T_g$ , reduced glass transition temperature  $T_{rg} = T_g/T_1$  and  $\gamma$  value ( $\gamma = T_x/(T_g + T_1)$ ) [31]. In this work, the absence of  $T_g$  means that  $\Delta T_x$ ,  $T_{rg}$ , and  $\gamma$  concepts cannot be employed to evaluate the GFA of the  $\text{Fe}_{48-x}\text{Co}_{27}\text{Zr}_3\text{Nd}_x\text{B}_{22}$  ( $x = 3-6$ ) alloys. However, as shown in Fig. 1, the proper addition of Nd (4–5 at.%) is very effective in improving the GFA.

It is interesting to note that the addition of Nd which exhibits positive enthalpy of mixing with Fe (+1 kJ/mol)

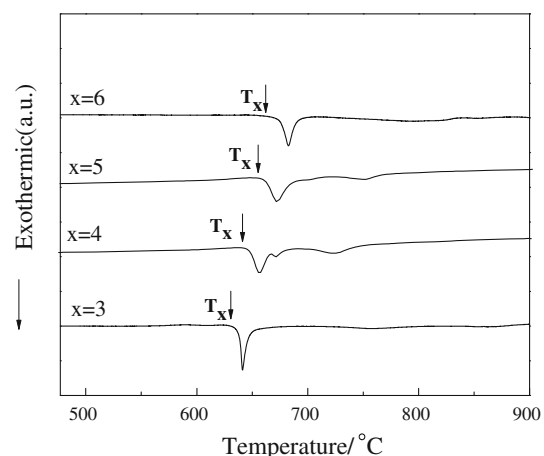


**Fig. 2** DSC curves of the  $\text{Fe}_{48-x}\text{Co}_{27}\text{Zr}_3\text{Nd}_x\text{B}_{22}$  ( $x = 3-6$ ) alloys prepared by suction casting

**Table 1** Values of  $T_x$ , grain size of magnetic phases, and magnetic property of  $Fe_{48-x}Co_{27}Zr_3Nd_xB_{22}$  ( $x = 3-6$ ) alloys

Component	$T_x$ (°C)	$M_s$ (Am <sup>2</sup> /kg)	$iH_c$ (kA/m)	$M_r$ (Am <sup>2</sup> /kg)	Grain size (nm)		
					Nd <sub>2</sub> Fe <sub>14</sub> B	$\alpha$ -Fe	FeB
$x = 3$	631	–	–	–	–	–	–
$x = 4$	640	76	51 (760 °C/10 min)	22	58	38	40
$x = 5$	656	57	179 (760 °C/10 min)	21	45	30	35
$x = 6$	662	–	–	–	–	–	–

and Zr (+10 kJ/mol) [32], results in GFA improvement, which is similar to Guo’s result [33]. The reason can be discussed from three aspects. First, Nd has large negative heat of mixing with Co (–24 kJ/mol) [34] and B (–49 kJ/mol) [35], which might help to maintain the stability of the liquid phase. Next, the chemical incompatibility in Nd–Fe pair and Nd–Zr pair is overcome by a positive atomic size effect. In the Fe–Co–Zr–Nd–B system, the addition of Nd element causes the more change in atomic size in the order of  $Nd > Zr > Co > Fe \gg B$ . The large atomic size mismatch: Zr–Nd 12%, Co–Nd 31%, Fe–Nd 30%, and B–Nd 50%. It is favorable for forming densely packed random structures with high thermal stability according to empirical rules [27]. Finally, as seen in Fig. 1, a small amount of Nd (4–5 at.%) can suppress the formation of  $\alpha$ -Fe phase. Being a rare earth element, the role is similar to that of Y in Zr-based alloy by suppressing the precipitation of the Zr<sub>2</sub>Ni laves phase [36].

**Bulk permanent magnets**

Based on the results of Figs. 1 and 2, we choose  $Fe_{44}Co_{27}Zr_3Nd_4B_{22}$  ( $x = 4$ ) and  $Fe_{43}Co_{27}Zr_3Nd_5B_{22}$  ( $x = 5$ ) alloys to study in detail. The XRD patterns for  $x = 4$  and  $x = 5$  alloys after annealing at 760 °C for 10 min are shown in Fig. 3. No appreciable difference in the crystallized phases is observed. The diffraction patterns

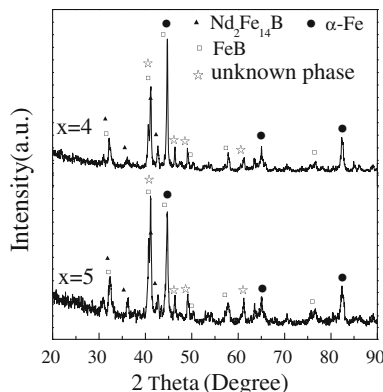


**Fig. 3** XRD patterns for annealed  $Fe_{44}Co_{27}Zr_3Nd_4B_{22}$  ( $x = 4$ ) and  $Fe_{43}Co_{27}Zr_3Nd_5B_{22}$  ( $x = 5$ ) samples at 760 °C for 10 min

are identified as  $\alpha$ -Fe, Nd<sub>2</sub>Fe<sub>14</sub>B, FeB, and an unknown phase. However, with increasing Nd addition up to 5 at.%, the relative diffraction peak intensities of hard magnetic Nd<sub>2</sub>Fe<sub>14</sub>B phase and unknown phase increase, while that of soft magnetic  $\alpha$ -Fe phase decrease. It is suggested that more Nd<sub>2</sub>Fe<sub>14</sub>B phase and the unknown phase form and less  $\alpha$ -Fe phase form in the  $Fe_{43}Co_{27}Zr_3Nd_5B_{22}$  alloy. The average grain size of hard magnetic and soft magnetic phases is calculated from the width of the diffraction peaks employing the Scherrer formula [37] and shown in Table 1, indicating that the annealed alloys consist of nanometer-sized crystallites.

The hysteresis loops of  $Fe_{44}Co_{27}Zr_3Nd_4B_{22}$  ( $x = 4$ ) and  $Fe_{43}Co_{27}Zr_3Nd_5B_{22}$  ( $x = 5$ ) alloys after annealing at 760 °C for 10 min are shown in Fig. 4a, b. For comparison, the hysteresis loops for as-cast sample is also included. It can be seen  $x = 4$  and  $x = 5$  alloys have similar magnetic behavior. That is, the as-cast samples exhibit soft magnetic property while present hard magnetic behavior after annealing at 760 °C. The hard magnetic properties are shown in Table 1.

It is noteworthy that saturation magnetization ( $M_s$ ) is 76 Am<sup>2</sup>/kg for  $x = 4$  alloy and 57 Am<sup>2</sup>/kg for  $x = 5$  alloy, respectively. Although some magnetic phases, such as

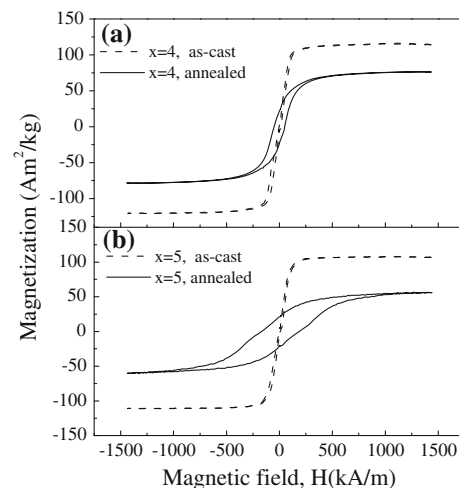


**Fig. 4** Hysteresis loops of as-cast and annealed  $Fe_{44}Co_{27}Zr_3Nd_4B_{22}$  ( $x = 4$ ) alloy (a) and  $Fe_{43}Co_{27}Zr_3Nd_5B_{22}$  ( $x = 5$ ) alloy (b) at 760 °C for 10 min

$\text{Nd}_2\text{Fe}_{14}\text{B}$ ,  $\alpha\text{-Fe}$ , and  $\text{FeB}$  phases, are presented after annealing at  $760\text{ }^\circ\text{C}$ , the values of  $M_s$  are not as high as expected (values of  $M_s$  for  $\alpha\text{-Fe}$ ,  $\text{Nd}_2\text{Fe}_{14}\text{B}$ , and  $\text{FeB}$  are 218, 160, and  $150\text{ Am}^2/\text{kg}$  [38], respectively). Therefore, a speculation can be made that the unknown phase is non-magnetic phase or magnetic phase with low saturation magnetization, which has less contribution to the magnetic property of annealed  $\text{Fe}_{44}\text{Co}_{27}\text{Zr}_3\text{Nd}_4\text{B}_{22}$  alloy and  $\text{Fe}_{43}\text{Co}_{27}\text{Zr}_3\text{Nd}_5\text{B}_{22}$  alloy. As Nd content increases from 4 to 5 at.%,  $M_s$  decreases from 76 to  $57\text{ Am}^2/\text{kg}$ , which is due to less formation of soft magnetic  $\alpha\text{-Fe}$  phase. Although the annealed alloys consist hard and soft magnetic phases, the smooth hysteresis loops without any steps are typical of a single-phase magnet. It is suggested that the hard magnetic properties can be interpreted to result from exchange magnetic coupling between nanometer-sized hard magnetic and soft magnetic phases. That is, bulk permanent magnets can be obtained by the simple process of copper mold casting and subsequent heat treatment. In addition, the value of coercivity ( $H_c$ ) for  $\text{Fe}_{43}\text{Co}_{27}\text{Zr}_3\text{Nd}_5\text{B}_{22}$  ( $x = 5$ ) alloy is  $179\text{ kA/m}$ , higher than that of  $\text{Fe}_{44}\text{Co}_{27}\text{Zr}_3\text{Nd}_4\text{B}_{22}$  alloy ( $51\text{ kA/m}$ ). There are two possible reasons. One is that the volume fraction of the  $\text{Nd}_2\text{Fe}_{14}\text{B}$  phase increases for the annealed  $\text{Fe}_{43}\text{Co}_{27}\text{Zr}_3\text{Nd}_5\text{B}_{22}$  alloy as shown in Fig. 3. The other is that smaller grain size of magnetic phases could enhance exchange magnetic coupling interaction.

It should be noted that the reduced remanence ( $M_r/M_s$ ) is less than 0.5, which is contrary to commonly reported in exchange-coupled type magnets. The possible reason is that non-ferromagnetic or weak-ferromagnetic unknown phases are in the coexistence with hard and soft magnetic phases, which may weaken the exchange coupling between soft and hard magnetic phases. Hence, the magnetic property of  $\text{Fe}_{48-x}\text{Co}_{27}\text{Zr}_3\text{Nd}_x\text{B}_{22}$  ( $x = 4\text{--}5$ ) alloys could be further improved if the minor addition and proper annealing treatment are properly chosen and controlled.

## Conclusion

In this study, proper addition of Nd (4–5 at.%) was very effective in improving GFA of Fe–Co–Zr–Nd–B alloys. The bulk amorphous  $\text{Fe}_{44}\text{Co}_{27}\text{Zr}_3\text{Nd}_4\text{B}_{22}$  and  $\text{Fe}_{43}\text{Co}_{27}\text{Zr}_3\text{Nd}_5\text{B}_{22}$  alloys were obtained. Especially, the as-cast  $\text{Fe}_{44}\text{Co}_{27}\text{Zr}_3\text{Nd}_4\text{B}_{22}$  and  $\text{Fe}_{43}\text{Co}_{27}\text{Zr}_3\text{Nd}_5\text{B}_{22}$  alloys exhibited soft magnetic behavior, while presented hard magnetic behavior after annealing at  $760\text{ }^\circ\text{C}$  for 10 min. That is, bulk  $\text{Fe}_{44}\text{Co}_{27}\text{Zr}_3\text{Nd}_4\text{B}_{22}$  and  $\text{Fe}_{43}\text{Co}_{27}\text{Zr}_3\text{Nd}_5\text{B}_{22}$  permanent magnets could be produced by the simple process of copper mold casting and subsequent heat treatment.

**Acknowledgements** The authors gratefully acknowledge the Instrumental Analysis & Research Center, Shanghai University. This study was sponsored by the National Natural Science Foundation of China (Grant No. 50671059) and Shanghai leading Academic Discipline Project (Grant No. S30107).

## References

- Johnson WL (1999) MRS Bull 24:42
- Inoue A (2000) Acta Mater 48:279
- Wang WH (2007) Prog Mater Sci 52:540
- Li CF, Zhang CJ (2009) J Mater Sci 44:4900. doi:10.1007/s10853-009-3748-5
- Scudino S, Surreddi KB, Sager S, Sakaliyska M, Kim JS, Löser W, Eckert J (2008) J Mater Sci 43:4518. doi:10.1007/s10853-008-2647-5
- Tekaya A, Labdi S, Benameur T, Jellad A (2009) J Mater Sci 44:4930. doi:10.1007/s10853-009-3752-9
- Luo XM, Zhou Y, Lu JQ, Yu GS, Lin JG, Li W (2009) J Mater Sci 44:4389. doi:10.1007/s10853-009-3661-y
- Xu Y, Wang YL, Liu XJ, Chen GL, Zhang Y (2009) J Mater Sci 44:3861. doi:10.1007/s10853-009-3523-7
- Cheng JB, Liang XB, Xu BS, Wu YX (2009) J Mater Sci 44:3356. doi:10.1007/s10853-009-3436-5
- Duwez P, Lin CH (1967) J Appl Phys 38:4096
- Hagiwara M, Inoue A, Masumoto T (1982) Metall Trans 13A:373
- Koshiba H, Inoue A, Makino A (1999) J Appl Phys 85:5136
- Inoue A, Shinohara Y, Gook SJ (1995) Mater Trans JIM 36:1427
- Inoue A, Zhang T, Takeuchi A (1997) Appl Phys Lett 71:464
- Chiriac H, Lupu N (1999) J Non-Cryst Solids 250:75112
- Inoue A (1999) Mater Trans JIM 40:643
- Chiriac H, Lupu N (2000) J Magn Magn Mater 215:394
- Shen BL, Inoue A, Chang C (2004) Appl Phys Lett 85:4911
- Inoue A, Shen BL (2004) Mater Sci Eng A375–A377:302
- Inoue A, Shen BL (2002) Mater Trans 43:766
- Zhang W, Inoue A (2002) Appl Phys Lett 80:1610
- Tan XH, Xu H, Bai Q, Dong YD (2007) J Non-Cryst Solids 354:410
- Tan XH, Xu H, Bai Q, Dong YD (2007) Appl Phys Lett 91:252501
- Tan XH, Xu H, Bai Q, Zhao WJ, Dong YD (2008) J Alloys Compd 452:373
- Chiriac H, Lupu N (2001) Phys B Condens Matter 299:293
- Pawlik P, Davies HA, Gibbs MRJ (2003) Appl Phys Lett 83:2775
- Inoue A (1997) Mater Sci Eng A 226:357
- Shen TD, Schwarz RB (1999) Appl Phys Lett 75:5
- Han Z, Zhang J, Li Y (2007) Intermetallics 15:1447
- Inoue A, Zhang W (2005) J Appl Phys 97:10H308
- Lu ZP, Liu CT (2002) Acta Mater 50:3051
- Park ES, Jeong EY, Lee JK, Bae JC, Kwon AR, Gebert A, Schultz L, Chang HJ, Kim DH (2007) Scr Mater 56:197
- Guo FQ, Poon SJ, Shiflet GJ (2004) J Appl Phys 97:013512
- Huang XM, Chang CT, Chang ZY, Wang XD, Cao QP, Shen BL, Inoue A, Jiang JZ (2008) J Alloys Compd 460:708
- Zhang J, Feng YP (2008) J Mater Res 24:357
- Wang WH, Bian Z, Wen P, Pan MX, Zhao DQ (2002) Intermetallic 10:1249
- Patterson A (1939) Phys Rev 56:978
- Giri L, Giri AK, Gonzalez JM (1995) Scripta Metall Mater 33:1725